

Journal Pre-proof

Linear epitope landscape of the SARS-CoV-2 Spike protein constructed from 1,051 COVID-19 patients

Yang Li, Ming-liang Ma, Qing Lei, Feng Wang, Wei Hong, Dan-yun Lai, Hongyan Hou, Zhao-wei Xu, Bo Zhang, Hong Chen, Caizheng Yu, Jun-biao Xue, Yun-xiao Zheng, Xue-ning Wang, He-wei Jiang, Hai-nan Zhang, Huan Qi, Shu-juan Guo, Yandi Zhang, Xiaosong Lin, Zongjie Yao, Jiaoxiang Wu, Huiming Sheng, Yanan Zhang, Hongping Wei, Ziyong Sun, Xionglin Fan, Sheng-ce Tao

PII: S2211-1247(21)00229-1

DOI: <https://doi.org/10.1016/j.celrep.2021.108915>

Reference: CELREP 108915

To appear in: *Cell Reports*

Received Date: 5 August 2020

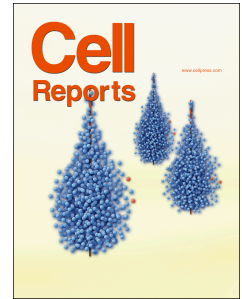
Revised Date: 3 February 2021

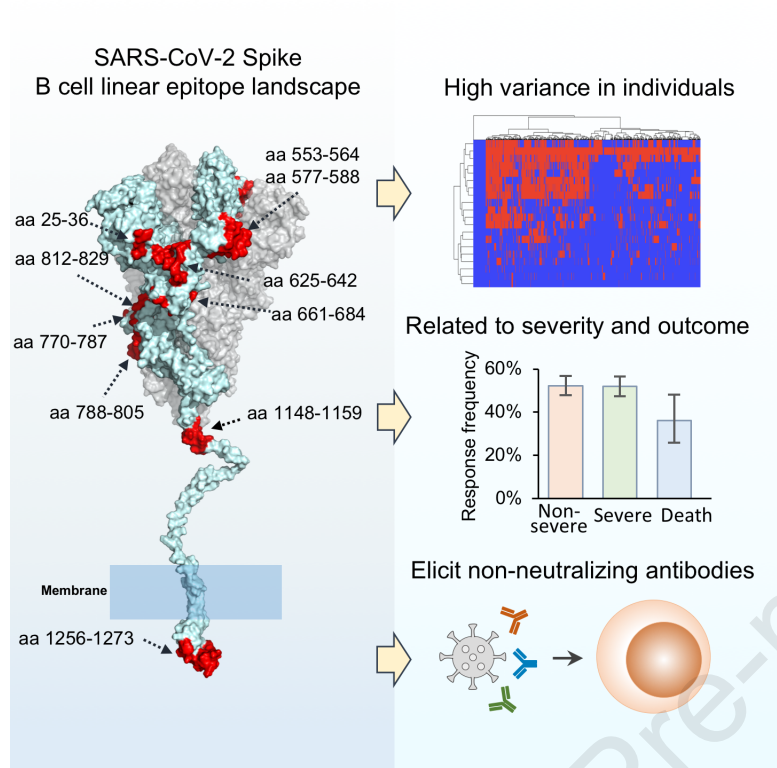
Accepted Date: 8 March 2021

Please cite this article as: Li, Y., Ma, M.-l., Lei, Q., Wang, F., Hong, W., Lai, D.-y., Hou, H., Xu, Z.-w., Zhang, B., Chen, H., Yu, C., Xue, J.-b., Zheng, Y.-x., Wang, X.-n., Jiang, H.-w., Zhang, H.-n., Qi, H., Guo, S.-j., Zhang, Y., Lin, X., Yao, Z., Wu, J., Sheng, H., Zhang, Y., Wei, H., Sun, Z., Fan, X., Tao, S.-c., Linear epitope landscape of the SARS-CoV-2 Spike protein constructed from 1,051 COVID-19 patients, *Cell Reports* (2021), doi: <https://doi.org/10.1016/j.celrep.2021.108915>.

This is a PDF file of an article that has undergone enhancements after acceptance, such as the addition of a cover page and metadata, and formatting for readability, but it is not yet the definitive version of record. This version will undergo additional copyediting, typesetting and review before it is published in its final form, but we are providing this version to give early visibility of the article. Please note that, during the production process, errors may be discovered which could affect the content, and all legal disclaimers that apply to the journal pertain.

© 2021 The Author(s).





1 **Linear epitope landscape of the SARS-CoV-2 Spike protein constructed**
2 **from 1,051 COVID-19 patients**

3
4 Yang Li^{1,5,9}, Ming-liang Ma^{1,9}, Qing Lei^{2,9}, Feng Wang^{3,9}, Wei Hong^{4,6,9}, Dan-yun Lai¹,
5 Hongyan Hou³, Zhao-wei Xu¹, Bo Zhang³, Hong Chen¹, Caizheng Yu⁷, Jun-biao Xue¹,
6 Yun-xiao Zheng¹, Xue-ning Wang¹, He-wei Jiang¹, Hai-nan Zhang¹, Huan Qi¹, Shu-juan
7 Guo¹, Yandi Zhang², Xiaosong Lin², Zongjie Yao², Jiaoxiang Wu⁸, Huiming Sheng⁸,
8 Yanan Zhang^{4,6}, Hongping Wei^{4,6*}, Ziyong Sun^{3,*}, Xionglin Fan^{2*}, Sheng-ce Tao^{1,10*}

9
10
11 ¹Shanghai Center for Systems Biomedicine, Key Laboratory of Systems Biomedicine
12 (Ministry of Education), Shanghai Jiao Tong University, Shanghai, China

13 ²Department of Pathogen Biology, School of Basic Medicine, Tongji Medical College,
14 Huazhong University of Science and Technology, Wuhan, China

15 ³Department of Clinical Laboratory, Tongji Hospital, Tongji Medical College, Huazhong
16 University of Science and Technology, Wuhan, China

17 ⁴CAS Key Laboratory of Special Pathogens and Biosafety, Centre for Biosafety
18 Mega-Science, Wuhan Institute of Virology, Chinese Academy of Sciences, Wuhan,
19 Hubei, China

20 ⁵College of Life Science, Nankai University, Tianjin 300071, China

21 ⁶University of Chinese Academy of Sciences, Beijing, China

22 ⁷Department of Public Health, Tongji Hospital, Tongji Medical College, Huazhong
23 University of Science and Technology, Wuhan, China.

24 ⁸Tongren Hospital, Shanghai Jiao Tong University School of Medicine, Shanghai, China

25

26 ⁹These authors contribute equally to this work.

27 ¹⁰Lead contact

28

29 * Corresponding Authors, e-mail: taosc@sjtu.edu.cn (S.-C. Tao), xlfan@hust.edu.cn (X.-L.
30 Fan), zysun@tjh.tjmu.edu.cn (Z.-Y. Sun) and hpwei@wh.iov.cn (H.-P. Wei).

31

32

33

34

35
36

37 **Summary**

38 To fully decipher the immunogenicity of the SARS-CoV-2 Spike protein, it is essential to
39 assess which part is highly immunogenic in a systematic way. We generate a linear
40 epitope landscape of the Spike protein by analysing the serum IgG response of 1,051
41 COVID-19 patients with a peptide microarray. We reveal two regions rich in linear
42 epitopes, *i.e.*, CTD and a region close to the S2' cleavage site and fusion peptide.
43 Unexpectedly, we find that the RBD lacks linear epitope. We reveal that the number of
44 responsive peptides is highly variable among patients and correlates with disease severity.
45 Some peptides are moderately associated with severity and clinical outcome. By
46 immunizing mice, we obtained linear-epitope-specific antibodies; however, no significant
47 neutralizing activity against the authentic virus was observed for these antibodies. This
48 landscape will facilitate our understanding of SARS-CoV-2-specific humoral responses
49 and might be useful for vaccine refinement.

50

51 **Keywords**

52 COVID-19, SARS-CoV-2, Spike protein, linear epitope landscape, neutralizing
53 antibodies

54

55

56

57

58

59

60

61

62

63

64

65

66 Introduction

67 COVID-19 is caused by SARS-CoV-2 (Wu et al., 2020b; Zhou et al., 2020b), which is
68 still causing an unfolding global pandemic. By February 3, 2021, 103,972,191 cases had
69 been diagnosed and 2,255,496 lives had been claimed
70 (<https://coronavirus.jhu.edu/map.html>) (Dong et al., 2020a). Recently, several COVID-19
71 vaccines have been successfully developed and approved by FDA (food and drug
72 administration) (Baden et al., 2020; Polack et al., 2020), and more candidates are on the
73 road (Dong et al., 2020b; Krammer, 2020). They will be undoubtedly helpful to combat
74 this pandemic. However, there are still several unelucidated immunological questions
75 related with SARS-CoV-2 infection that need much more effort to answer to benefit
76 disease therapy as well as refinement of vaccine design (Jeyanathan et al., 2020).

77

78 The genome of SARS-CoV-2 encodes 27 proteins, and among them, the Spike protein
79 plays a central role in the binding and entry of the virus to the host cell. The Spike protein
80 is cleaved into S1 and S2 at furin and S2' sites by specific proteases (Andersen et al.,
81 2020). The Spike protein is highly glycosylated with 21 N-glycosylation sites (Watanabe
82 et al., 2020). The Spike protein, and more specifically the RBD domain, is currently the
83 target most focused on for the development of COVID-19 neutralizing antibodies and
84 vaccines (Baum et al., 2020; Cao et al., 2020; Hansen et al., 2020a; Wec et al., 2020; Wu
85 et al., 2020d; Yuan et al., 2020a). Actually, RBD is immunodominant to elicit
86 SARS-CoV-2 specific antibodies and RBD IgG response highly correlates with the S1
87 subunit IgG level (Jiang et al., 2020a; Premkumar et al., 2020), and importantly, RBD
88 antibody level also highly correlates neutralizing activities of sera from patients (Iyer et
89 al., 2020; Premkumar et al., 2020).

90

91 Out of RBD, other regions of Spike or S1 subunit can also elicit strong antibodies
92 (Shrock et al., 2020; Wang et al., 2020a) and some epitopes elicited antibodies have been
93 demonstrated to exhibit neutralizing activities (Chi et al., 2020; Li et al., 2020a; Poh et al.,

94 2020). However, fully investigation of the Spike epitopes that can elicit antibodies, in
95 particular neutralizing antibodies has been not reported. Furthermore, if the epitopes elicit
96 non-neutralizing antibodies, what the beneficial or detrimental functions in disease
97 development or vaccination is also poorly understood. Despite beneficial function of any
98 virus binding antibody due to ADCC (antibody dependent cellular cytotoxicity) effect to
99 help to eliminate pathogens, ADE (antibody dependent enhancement) and
100 pro-inflammation caused by antibodies are unneglectable concerns (Liu et al., 2019;
101 Vabret et al., 2020). Although whether ADE occurs in the context of SARS-CoV-2
102 infection remains unclear, the facts that higher antibody titers and neutralizing plasm
103 activities in patients are associated more severe conditions (Jiang et al., 2020a; Long et
104 al., 2020a) and cytokine profiles resemble those in macrophage activation syndrome
105 (Jeyanathan et al., 2020; Mehta et al., 2020) warrants further investigation of ADE as
106 well as VAED (vaccine-associated enhanced disease) (Haynes et al., 2020). In addition,
107 non-neutralizing antibodies may compete with and suppress the neutralizing antibody
108 production through a widely studied mechanism called immunodominance (Abbott and
109 Crotty, 2020; Cirelli et al., 2019). So non-neutralizing antibodies should be avoided to
110 maximum the production of neutralizing antibody as well as minimize the likelihood of
111 disease enhancement for vaccine design (Abbott and Crotty, 2020; Jeyanathan et al.,
112 2020). Collectively, elucidation of high antigenic epitopes and investigation of the
113 neutralization property of these epitopes is quite essential to refine vaccine design.

114

115 In the present study, through a large cohort of COVID-19 patients and controls, we build
116 a full linear epitope landscape of B cells against SARS-CoV-2 spike protein, identifying
117 that CDT on S1 unit and FP region on S2 unit are two antigenic hot arear while RBD
118 lacks linear epitopes. Combined with tensive clinical data, we found responsive epitope
119 numbers and some specific linear epitopes are associated with disease severity. No
120 neutralizing activities were detected for the antibodies elicited by the linear peptides
121 immunized in mice.

122

123 **Results**

124 **The IgG linear epitope landscape of the SARS-CoV-2 Spike protein**

125 To reveal the immunogenic linear epitopes of the Spike protein, a peptide microarray
126 with full coverage of the Spike protein was updated from an original version (Li et al.,
127 2020a). Since B cell linear epitopes for antibody recognition typically span 3-8
128 continuous amino acids (aa) (Larman et al., 2011; Shi et al., 2019) and peptides of 10-12
129 aa are commonly used for immunization to develop antibodies (Wang et al., 2020c), to
130 largely cover possible linear epitopes, we synthesized peptides of 12 aa with 6 aa overlap
131 for every two adjacent peptides. A total of 211 peptides across the S protein were selected
132 (**Fig. S1, Table S1**). Sera were collected from two groups, 1,051 COVID-19 patients and
133 528 controls (**Table S2**), and individually analysed on the peptide microarray. By plotting
134 the signal intensities of all the samples against each peptide, a linear epitope landscape
135 was constructed; for a better overview, the landscape was aligned to the sequence of the
136 Spike protein (**Fig. 1**). To assure specificity, all the control samples (**Table S2**) were also
137 analysed on the peptide microarray. Almost all the peptides were negative for all the
138 control samples, while significant binding was observed for many of the peptides when
139 probed with COVID-19 sera. This indicates that the positive bindings are SARS-CoV-2
140 specific.

141 To determine which epitopes were highly immunogenic, the criteria were set as an
142 average_signal intensity greater than $3 \times \text{Cutoff2}$ and a response frequency greater than 10%
143 (see methods for the definitions). A total of 16 peptides were obtained; surprisingly, all of
144 them are outside of the RBD. We hereby define these peptides or epitopes as significant
145 epitopes. Due to the significance of the RBD, we lowered the criteria, *i.e.*, a response
146 frequency greater than 1%, while keeping the average_signal intensity greater than
147 $3 \times \text{Cutoff2}$. Three consecutive epitopes of moderate immunogenicity, S1-76, S1-77 and
148 S1-78, were selected (**Table S3**). Interestingly, all three epitopes were located within the
149 RBM (receptor binding motif), the binding interface of the Spike protein and ACE2.

150 While a few of these immunogenic epitopes are dispersed on the Spike protein, there
151 are two linear epitope “hot” regions that could be immediately recognized: aa525-685
152 and aa770-829, one of which is the CTD (C-terminal domain) and another that covers the
153 S2' cleavage site and the fusion peptide (FP). There are several SARS-CoV-2
154 epitope-related studies involving small sample sets (Ahmed et al., 2020; Wang et al.,

155 2020b). Our immunogenic epitopes are partially consistent with these studies (**Table S3**).
156 A relative high consistency was observed between our data, ReScan and VirScan, a
157 phage display-based strategy (Shrock et al., 2020; Xu et al., 2015; Zamecnik et al., 2020).

158 To further illustrate the location and distribution of the 19 immunogenic epitopes
159 (**Table S3**), we mapped them to the 3D structure of the Spike protein (Herrera et al., 2020)
160 (**Fig. S2A, S2B** and **Table S4**). It is clear that most of these epitopes were located on the
161 surface of the Spike protein, which is consistent with the common idea (Emeni et al.,
162 1985). Additionally, an accessibility analysis at the amino-acid level revealed that most
163 epitopes have at least 5 accessible amino acids on the trimer of the Spike protein and
164 more on the monomer (**Fig. 1B** and **Fig. S2C**). For S1-111, S2-16, S2-18 and S2-19,
165 there are substantially fewer accessible amino acids on the trimer than on the monomer.
166 A plausible explanation is that the Spike protein monomer could be exposed to the
167 immune system at a certain, yet-to-be discovered stage. In addition, except for S1-77/78
168 on RBD, no big difference of the accessible amino acid numbers was observed for other
169 epitopes in open and close state of Spike trimer (data not shown). For the immunogenic
170 epitopes (**Table S3**), the solubility (Kyte and Doolittle, 1982) and isoelectric point (pI)
171 range from -1.97 to 1.06 and 3.01 to 11.16, respectively, and the hydrophilicity and pI of
172 the epitopes are not correlated with response frequency (**Fig. S1D, E**).

173 It was speculated that the N-glycosylation may interfere with antibody responses
174 (Sikora et al., 2020). To test this speculation, we divided all the peptides into two groups:
175 with or without an N-glycosylation site. We found that there was no significant decrease
176 in response frequency for the group with glycosylation compared to the group without
177 glycosylation (**Fig. 1C**), suggesting that the distribution of the linear epitope is not or is
178 only subtly related to N-glycosylation.

179 It is interesting to examine if there is any correlation among different epitopes and
180 epitopes vs. the S protein. To answer this question, we tested the independence of IgG
181 response among the significant epitopes. Taking S1-93 as an example, we found
182 significant correlations for almost all of the epitopes to S1-93, including S1 protein (**Fig.**
183 **1D**). Similar results were observed for other epitopes (**Fig. S3A, B**). These results suggest
184 that the IgG responses among the epitopes are correlated. Interestingly, although the
185 epitopes with high response frequencies are significantly correlated with each other, the

186 epitopes derived from the CTD region tend to have higher correlations with each other,
187 while this is not the case for the epitopes derived from the FP region (**Fig. 1E**).
188 Consistently, the heatmap of hierarchical-cluster analysis of IgG response signatures in
189 COVID-19 patients revealed associations among the significant epitopes (**Fig. S3C**). It
190 also demonstrated high variability among individual, which is consistent with the concept
191 that immune responses vary greatly from person to person (Boyd and Jackson, 2015; Li
192 et al., 2020b).

193

194 **Responsive epitopes correlate with the IgG response of the S protein and disease** 195 **severity**

196 To further investigate how SARS-CoV-2 S protein-specific IgG responses vary among
197 COVID-19 patients, we counted the total numbers of responsive epitopes in each sample.
198 It is known that the antibody response against SARS-CoV-2 reaches a plateau
199 approximately two weeks after symptom onset (Long et al., 2020). To maintain
200 consistency in antibody responses, only samples collected 15 days or more after symptom
201 onset were analysed. The average number of responsive epitopes in the patient group are
202 greater than those in the control group, *i.e.*, 7.6 vs. 1.2, respectively. However, the
203 numbers are highly variable among individuals (**Fig. 2A, B**). We next tested whether the
204 responsive epitopes are related to severity. We divided the patients into three groups
205 concerning severity and final outcome, *i.e.*, non-severe (mild and moderate), severe
206 survivors (severe and critical) and severe non-survivors (death). The numbers in the
207 severe groups are significantly higher than those in the non-severe group (8.2 vs. 7.1 in
208 average), while there is no significant difference between non-survivors and severe
209 survivors (**Fig. 2C**). In addition, the number of responsive epitopes highly correlates with
210 S protein IgG (**Fig. 2D**). This observation demonstrates that S protein-derived responsive
211 epitopes contribute to immune responses to the S protein, which is expected.

212 We next analysed the possible correlation between the epitopes and disease severity. In
213 general, there is no obvious difference among the three groups (**Fig. 3A**), except some
214 epitopes and the S1 protein, which correlates with severity and/or outcome (**Fig. 3B-E**,
215 **Table S5**). Particularly, for S1-93, S1-97 and S2-78, a statistically significant decrease in
216 the IgG response in the non-survivor group was observed (**Fig. 3C-E**), suggesting

217 protective roles for the corresponding antibodies. Consistently, the IgG response to the
218 epitopes correlated with clinical parameters related to disease severity (Huang et al., 2020;
219 Wu et al., 2020a), such as LDH, C reactive protein and lymphocyte percentage (**Table**
220 **S6**). There were a few epitopes that were related to gender (**Table S5**) or age (**Table**
221 **S5**). In particular, S1-5 and S1-97, as well as S1 protein were significantly associated
222 with age, which was consistent with our previous study with a small cohort (Jiang et al.,
223 2020a). Although NAT (nuclear acid test) positivity is the gold standard for diagnosis,
224 antibody tests or other approaches might be essential and complementary (Long et al.,
225 2020a, 2020b). In our cohort, there are 248 clinically confirmed cases that were NAT
226 negative. For this group of cases, the S1 IgG response prevalence is also high, though it is
227 lower than that of the NAT-positive group (**Table S5**), while the antibody response levels
228 against the significant epitopes were similar for both the NAT-positive and negative
229 groups (**Table S5**).

230

231 **RBD lacks linear epitopes, while it is highly immunogenic**

232 It is well known that the RBD is highly immunogenic (Jiang et al., 2020a; Premkumar et
233 al., 2020). However, according to our selection criteria, no highly immunogenic epitope
234 was obtained from the RBD. Only when we lowered the selection criteria were 3 peptides
235 selected, S1-76, S1-77 and S1-78 (**Fig. 4A**). When the RBD is compared to other regions
236 of the Spike protein, it is obvious that the RBD has very poor in linear epitopes. This
237 seems contradictory to the knowledge that the RBD is highly immunogenic. It is possible
238 that most of the epitopes of the RBD region are conformational. To test this possibility,
239 we collected a set of 9 high affinity monoclonal antibodies for the RBD or the Spike
240 protein (see methods). These antibodies were obtained through memory B cell isolation
241 from COVID-19-recovered patients (Wan et al., 2020). We analysed these antibodies
242 individually on the Spike protein peptide microarray (Li et al., 2020a) (**Fig. 4B**). Among
243 these antibodies, 414-1 has the highest affinity (2.96 nM) to the RBD. As expected,
244 strong bindings were observed for both the S1 protein and the RBD; however, negative
245 signals were obtained for all the peptides, including the RBD peptides from aa331-524.
246 Additionally, no peptide bindings were observed for the rest of the RBD-specific
247 antibodies (data not shown). For antibody 414-4, strong binding was obtained for the S1

248 protein but not for the RBD. Interestingly, 414-4 binds S1-97 with high affinity,
249 indicating the epitope that 414-4 recognizes is near aa577-588.

250 Actually, the 3 immunogenic epitopes, S1-76, S1-77 and S1-78, were also identified in
251 other related studies (Wang et al., 2020b; Zhang et al., 2020a). These three epitopes are
252 consecutive and located in the RBM region, which at least partially overlaps with or is
253 close to the binding epitopes of a variety of SARS-CoV-2 neutralizing antibodies, *e.g.*,
254 B38 (Wu et al., 2020d), CB6 (Shi et al., 2020) and P2B-2F6 (Ju et al., 2020). To further
255 illustrate these epitopes' locations, we mapped them to the 3D structure of the Spike
256 protein in both the open state and the closed state (**Fig. 4C**). In the closed state,
257 aa455-465 of S1-76/77/78 is located in the contact area among the three monomers and is
258 probably difficult to access, aa452-454 and 473-474 form the β -strand and are covered
259 but could be accessed from both sides, and only aa466-472 is exposed and present as a
260 flexible sequence (**Fig. 4D** and **Fig. S4**). In the open state of the Spike protein, all
261 residues of S1-76/77/78 are exposed and highly accessible (**Fig. S4**). To further analyse
262 the immunogenicity of S1-76/77/78, we examined all the available neutralizing
263 antibody-RBD complexes by the end of November 30th, 2020 as far as we know. (**Table**
264 **S7**). The antibodies are CB6 (Shi et al., 2020), P2B-2F6 (Ju et al., 2020), BD23 (Cao et
265 al., 2020), CR3022 (Yuan et al., 2020a), S309 (Pinto et al., 2020), CV30 (Hurlburt et al.,
266 2020), BD-368-2 (Du et al., 2020), CC12.1 (Yuan et al., 2020b), H11-D4 (PDB: 6YZ5),
267 REGN10933 (Hansen et al., 2020b), Fab2-4 (Liu et al., 2020), EY6A (Zhou et al., 2020a),
268 H014 (Lv et al., 2020), Ty1 (Hanke et al., 2020), MR17 (PDB: 7C8W), C105 (Hanke et
269 al., 2020), COVA2-04, COVA2-39 (Wu et al., 2020c), COVA1-16 (PDB: 7JMW),
270 S2E12, S2M11 (Tortorici et al., 2020), S2A4, S2H13, S2H14 (Piccoli et al., 2020),
271 CV07-250, CV07-270 (Kreye et al., 2020), C110, C119, C002, C135, C121, C102, C144
272 (Barnes et al., 2020), Fab-52, Fab-298 (Rujas et al., 2020), Nb6 (Schoof et al., 2020) and
273 Sb23 (Custódio et al., 2020). Among these structures, CB6, P2B-2F6, CV30, DB-368-2,
274 CC12.1, H11-D4, REGN10933, Fab2-4, Ty1, MR17 and C105 interact directly with
275 residues within S1-76/77/78. For the CB6-RBD complex, there are several residues
276 within S1-76/77/78 that directly interact with the following antibodies: Y453, L455, F456,
277 R457, K458, S459, N460, Y473 and Q474. The same interaction residues between
278 neutralizing antibodies and the RBD can also be found in the CV30-RBD, CC12.1-RBD

279 and C105-RBD complexes (**Table S7**). Partial interaction residues of the CB6-RBD
280 complex between S1-76/77/78 can also be found in the REGN10933-RBD,
281 H11-D4-RBD, Fab-2-4-RBD, Ty1-RBD and MR107-RBD complexes, and some other
282 residues, such as L452, T470 and I472, can be found in some of these structures (**Table**
283 **S7**). For the P2B-2F6-RBD complex, the only residue that directly interacts with the
284 antibody is L452. In summary, most of these neutralizing antibodies interact with
285 residues located in S1-76/77/78, residues 452-460 and 470-474 play direct roles in the
286 interactions, and the flexible loop consisting of residues 461-469 is irrelevant to these
287 neutralizing antibodies.

288 Broad neutralizing antibodies and a vaccine effective for SARS-CoV-2 and other
289 human coronaviruses are of high interest (Jiang et al., 2020b). We performed a homology
290 analysis for S1-76/77/78 among SARS-CoV-2, the other 6 human coronaviruses, and bat
291 coronavirus BtCoV-RaTG13 (Zhou et al., 2020b). High homologies were observed for
292 the all 3 epitopes among SARS-CoV-2, SARS-CoV and BtCoV-RaTG13 while low
293 homology level with MERS-CoV and other common coronavirus (**Figure 4E**). The high
294 homology indicates that antibodies elicited by S1-76/77/78 may at least be effective for
295 both SARS-Cov-2 and SARS-CoV.

296 These results strongly suggest that the RBD is rich in conformational epitopes, while it
297 lacks linear epitopes. The underlying mechanism is worth further investigation.

298

299 **CTD is rich in linear epitopes**

300 The first “hot” region of linear epitopes is CTD. The whole domain is densely covered by
301 linear epitopes (**Fig. 5A**). According to the selection criteria, 6 highly immunogenic
302 epitopes, S1-93, S1-97, S1-105/106, S1-111 and S1-113, were identified. These epitopes
303 are nearly evenly distributed across CTD. We then asked whether these 6 highly
304 immunogenic epitopes were also revealed in other studies. It showed that S1-93 was
305 identified by ReScan (Zamecnik et al., 2020) (**Table S3**), as well as COVIDep (Ahmed et
306 al., 2020), S1-97 by ReScan, and S1-111 by COVIDep.

307 S1-93 and S1-97 are located at CTD1, while aa555-564 of S1-93 and aa578-584 of

308 S1-97 are present at the loop region and on the surface of the trimeric Spike protein.

309 S1-105, S1-106, S1-111, and S1-113 are located at CTD2; S1-105/106 are almost at the

310 loop and present on the surface; S1-111 is at β -strand and the loop but buried inside; and
311 only aa667-669 on the loop region could be accessed. S1-113 is near the S1/S2 cleavage
312 site. Although aa677-684 is invisible in the Spike protein structure, these residues could
313 be exposed on the surface and induce an antibody response to prevent S1/S2 hydrolysis
314 (**Fig. 5B**). S1-113 is also on the outer surface, while S1-111 is on the inner surface, and
315 the underlying mechanism by which S1-111 triggers a strong IgG reaction in many
316 patients is worth further study.

317 Homology analysis was performed for the 6 highly immunogenic epitopes (**Fig. 5C**).
318 Except for S1-113, high homologies were observed for all 5 epitopes among
319 SARS-Cov-2, SARS-CoV and BtCoV-RaTG13 while lower homology levels were
320 shown among SARS-CoV-2 and MERS-CoV and the other four common coronaviruses.
321 The high homology indicates that antibodies elicited by S1-93, S1-97, S1-105 and S1-111
322 may be effective for both SARS-Cov-2 and SARS-CoV. Additionally, an antibody
323 targeting S1-113 may be specific for SARS-CoV-2.

324 The D614G mutant is the current dominant strain in Europe (Korber et al., 2020),
325 which has about a 9 times higher infection efficiency in cell assays than that of the
326 wild-type strain (Zhang et al., 2020b). D614 is within S1-102, an epitope of moderate
327 immunogenicity, and close to the highly immunogenic S1-105. Blocking the D614 region
328 may cause a functionally significant effect.

329
330 **The second epitope hot region spans aa770-829, covering the S2' cleavage site and**
331 **FP**

332 The second region with highly enriched linear epitopes spans aa770-829 (**Fig. S5A**).
333 According to the selection criteria, 6 highly immunogenic epitopes were obtained: S2-15,
334 S2-16, S2-18, S2-19, S2-22 and S2-23.

335 It is interesting to see whether these 6 highly immunogenic epitopes were also
336 identified in related studies. We revealed that S2-22 was identified by a peptide
337 microarray study (Wang et al., 2020b). Four epitopes (S2-18, S2-19, S2-22 and S2-23)
338 were identified by ReScan (Zamecnik et al., 2020), and 2 epitopes (S2-22 and S2-23)
339 were predicted by COVIDep (Ahmed et al., 2020). Of these epitopes, S2-22 is the only
340 one that was identified or predicted in all these studies. Since S2-22/23 covers the S2'

341 cleavage site and FP, we speculate that an antibody targeting S2-22/23 may block the
342 cleavage and disturb the function of FP; thus, it has potent neutralization activity.
343 Interestingly, a strong S2-22-specific IgG reaction was also elicited by an mRNA vaccine
344 study (Cai et al., 2020), which further demonstrated the high immunogenicity and high
345 potential of the neutralization activity of S2-22.

346 To further illustrate these epitopes' locations, we mapped them to the 3D structure of
347 the Spike protein. S2-15, S2-16, S2-18, S2-19, S2-22 and S2-23 are all located near the
348 S2' site and the FP region. aa770-783 of S2-15/16 forms an α -helix and is buried at the
349 trimer interface but is accessible on the monomer. aa791-805 of S2-18/19 forms a loop,
350 and aa816-826 forms a α -helix and is located on the surface. The S2' cleavage site is on
351 S2-22 (**Fig. S5B**).

352 To check the similarity of the epitopes among human coronaviruses, we performed a
353 homology analysis for S2-22/23, S2-15/16 and S2-18/19. High homologies were
354 observed for all these epitopes among SARS-Cov-2, SARS-CoV and BtCoV-RaTG13,
355 while only for S2-22/23, high homology was shown among SARS-CoV-2 and other
356 common coronaviruses (**Fig. S5C**). Interestingly, S2-22/23 is highly homologous among
357 all the coronaviruses and almost identical among SARS-Cov-2, SARS-CoV and
358 BtCoV-RaTG13.

359

360 **Other highly immunogenic linear epitopes**

361 Except for the immunogenic epitopes that belong to the RBD and the two "hot" regions,
362 there are other highly immunogenic epitopes dispersed across the Spike protein (**Fig.**
363 **S6A**). S1-5 is located at NTD, and part of the residues, *i.e.*, aa28-31, form the β -strand
364 and are on the surface of the trimeric Spike protein. aa32-36 forms a loop and is partially
365 covered by the other region. S2-78, S2-96 and S2-97 are located in unobserved regions in
366 the C-terminus of the Spike protein. We applied a modelling structure to present these
367 unobserved regions (**Fig. S6B**). S2-78 is predicted to be an α -helix, and S2-96/97 is
368 predicted to be a loop. S2-96/97 are at the very C-terminal end of the Spike protein (**Fig.**
369 **S6B**), which is located in the cytoplasm of the host cell.

370 We checked whether these 4 highly immunogenic epitopes were also revealed in other
371 studies. We found that S1-5 was identified by a peptide microarray study (Wang et al.,

2020b). S2-78 was identified by ReScan (Zamecnik et al., 2020), and 3 epitopes (S2-78, S2-96, S2-97) were predicted by COVIDep (Ahmed et al., 2020). The functional role of S1-5-specific antibodies may be worth further investigation. S2-78 is adjacent to HR2, and the antibody targeting this site may block the conformational change that is essential for effective virus-cell fusion (Liu et al., 2004). It is surprising to see the high immunogenicity of S2-96 and S2-97 since they are at the very C-terminal end of the Spike protein and theoretically localize in the cytoplasm. Further study is necessary to explore the underlying mechanism and functional roles of these epitopes.

High homologies were observed for all the epitopes among SARS-Cov-2, SARS-CoV and BtCoV-RaTG13 (**Fig. S6C**). Interestingly, S2-78 and S2-96/97 are highly homologous among all the coronaviruses and almost identical among SARS-Cov-2, SARS-CoV and BtCoV-RaTG13. For S2-78, a high homology was also observed for MERS-CoV.

385

386 **Antibody responses against most of the linear epitopes dramatically decrease after** 387 **reaching the peak**

We next assessed the longevity of the antibodies elicited by the linear epitopes. For the hospitalized patients listed in **Table S2**, longitudinal sera samples were collected. We define collection_time as the days from symptom onset to sample collection, and the collection_time is widely distributed from 1 to 60 (**Fig. S7A**). There are > 20 samples/day for collection_time ranging from 12 to 54 days, and > 50 samples/day for collection_time ranging from 20 to 45 days. To fully understand the trend dynamics in the IgG to the significant epitopes, the median signal intensities and response frequencies of the epitopes were calculated and plotted according to the collection_time. The S1 protein was included as a reference for this analysis. Surprisingly, while S1 IgG slowly decreases when collection_time is approximately 40 days (**Fig. 6A**), the antibodies against most of the epitopes dramatically decrease when collection_time is approximately 30 days (**Fig. 6C-G**). However, for the antibodies against S2-78, the linear epitope of the highest frequency, no significant decrease was observed for both the median signal intensity and the response frequency (**Fig. 6B**). This result is similar to that for S1 (**Fig. 6A**). Consistently, the trend in the median number of responsive epitopes is similar to that

403 of the S1 protein (**Fig. S7B, C**). These observations suggest that a decrease in or
404 disappearance of the antibodies against some epitopes may contribute to a decrease in S1
405 IgG antibodies, while the antibodies against some other epitopes could last longer.

406

407 **Antibodies from mice immunized with the linear peptides exhibit no significant** 408 **neutralization activity**

409 Although the RBD region is the essential part contributing to the neutralization activity of
410 S protein-elicited antibodies, other regions of the S protein are frequently reported to be
411 able to elicit neutralizing antibodies (Chi et al., 2020), including linear epitopes (Li et al.,
412 2020a; Poh et al., 2020). However, the entire spectrum showing which parts can and
413 which parts cannot elicit neutralizing antibodies has barely been elucidated. To fully
414 investigate the potential to elicit a neutralizing antibody using significant epitopes, the
415 most physiologically relevant method is to enrich specific antibodies from COVID-19
416 sera using the significant epitopes and then run a neutralization assay (Li et al., 2020a).
417 However, for antibody enrichment, a large volume of each serum sample is required, and
418 it is extremely difficult to collect more COVID-19 samples in large volumes at this time.
419 Alternatively, we tested whether the significant linear epitopes could elicit neutralizing
420 antibodies in a mouse model. When selecting overlapping peptides, we chose one with a
421 higher response frequency, except when both peptides were of a high response frequency.
422 For example, S1-78 was selected to represent the RBD. In total, 14 peptides were
423 selected. The peptides were conjugated to KLH, and 3 mice were immunized for each
424 peptide (**Fig. 7A**). Most of the linear epitopes elicited specific antibodies (**Fig. 7B**). Next,
425 we performed neutralization assays on the authentic SARS-CoV-2 virus with sera
426 collected from the immunized mice. Our results showed that some sera have marginal
427 neutralization activities (**Fig. 7C, D**) while no neutralization activity was observed for the
428 rest of the sera. The antibodies generated by S1-78, which is located squarely in the RBM
429 region, recognize the RBD protein (**Fig. 7B**) and are assumed to have high neutralization
430 activity. Unfortunately, significant neutralization activity was not observed, suggesting
431 the lower efficacy of linear peptide immunization antibodies (Zhang et al., 2020a). These
432 results suggest that significant epitopes may not be suitable for vaccine development

433 because of the very limited neutralization activities; thus, our results further strengthen
434 the central role of RBD for eliciting the neutralizing antibody.

435

436 **Discussion**

437 Herein, we aim to reveal IgG responses triggered by the SARS-CoV-2 Spike protein on a
438 systematic level. We adopted a newly developed peptide microarray with full coverage of
439 the Spike protein (Li et al., 2020a) and analysed 1,051 COVID-19 sera and 528 control
440 sera. A set of highly immunogenic epitopes were revealed, and a comprehensive IgG
441 linear epitope landscape was constructed.

442 One limitation of this study is that only short peptides were involved. Though linear
443 epitopes are nicely represented, conformational epitopes may not be. For example, for the
444 RBD region, which is highly immunogenic, only 3 linear epitopes of moderate
445 immunogenicity were identified. To overcome this limitation, one method is to
446 synthesize longer peptides, which may retain some conformational information (Zhang et
447 al., 2020a). It is necessary to note that for the linear epitopes we identified, they are
448 highly physiologically relevant as all of them were revealed through analysing sera from
449 COVID-19 patients.

450 Our study presents the first IgG linear epitope landscape of the Spike protein, which
451 could only be achieved by analysing a large cohort of samples using a systematic
452 approach, such as the full-coverage peptide microarray of the Spike protein. According to
453 the landscape, it is obvious that the Spike protein is highly immunogenic, there are many
454 epitopes on the protein, and these epitopes are not evenly distributed across the Spike
455 protein.

456 Using sera from peptide-immunized mice, we examined the ability of the linear
457 epitopes to elicit neutralization activity with the intact SARS-CoV-2 virus. However,
458 significant neutralization activity was not observed. Our previous studies and those of
459 other groups have identified some linear epitopes that can elicit neutralizing antibodies
460 (Li et al., 2020a; Poh et al., 2020). One plausible reason for this inconsistency is that
461 although the neutralization activities of the responsive epitope-elicited antibodies are very
462 low, a much higher concentration of antibodies is needed to demonstrate obvious
463 neutralization activity. To support this explanation, for the three antibodies enriched from

464 patient sera by S1-93, S1-105 and S2-78 that demonstrate neutralization activities, the
465 estimated IC₅₀ is approximately 5- 20 µg/mL (Li et al., 2020a), which is much higher
466 than that for the RBD-targeting antibodies isolated from COVID-19 patients (Cao et al.,
467 2020; Ju et al., 2020). In addition, linear peptide-directed immunization might not
468 effectively generate “valid” antibodies in vivo since the conformation of the peptide
469 might differ from that in the native Spike protein. Furthermore, this result is consistent
470 with the study in which RBD-derived peptides were used for the immunization of mice
471 (Zhang et al., 2020a).

472 Our results can be used to examine the hypotheses regarding the relationship between
473 SARS-CoV-2-specific humoral responses to linear spike peptides and the elicitation and
474 recognition of neutralizing antibodies. In other words, the antibodies against the highly
475 immunogenic linear epitopes have less or very limited neutralization activities against
476 SARS-CoV-2. Thus, when applying the S protein for vaccination, it may be necessary to
477 block or remove some of the immunodominant linear epitopes that we identified to
478 improve the efficacy and avoid possible side effects.

479 Taken together, we built a comprehensive linear epitope landscape that covers the
480 entire sequence of the SARS-CoV-2 Spike protein by using sera from 1,051 COVID-19
481 patients. A set of 16 highly immunogenic epitopes outside of the RBD region were
482 identified. The antibody responses against several epitopes are associated with severity.
483 Little neutralization activity was observed for the antibodies against the highly
484 immunogenic epitopes. These findings facilitate our understanding of the humoral
485 immunity of SARS-CoV-2 on a systems level, which may provide some directions for the
486 refinement of COVID-19 vaccine design.

487

488 **Acknowledgements:**

489 We thank Dr. Daniel M. Czajkowsky for critical reading and editing. We thank Prof.
490 Zhengfan Jiang from the Key Laboratory of Cell Proliferation and Differentiation of the
491 Ministry of Education School of Life Science, Peking University for kindly providing the
492 manganese salt (MnJ) adjuvant. We also thank Prof. Jing-Hua Yan at the Institute of
493 Microbiology, Chinese Academy of Sciences for kindly providing the CB6 antibody.
494 This work was partially supported by the National Key Research and Development

495 Program of China Grant (No. 2016YFA0500600), the Science and Technology
496 Commission of Shanghai Municipality (No. 19441911900), the Interdisciplinary Program
497 of Shanghai Jiao Tong University (No. YG2020YQ10), the National Natural Science
498 Foundation of China (No. 31970130, 31600672, 31670831, and 31370813) and China
499 Postdoctoral Science Foundation (No. 2020M680857).

500

501 **Author contributions:**

502 S-C. T. developed the conceptual ideas and designed the study. Z-Y. S., F.W., H-Y. H.,
503 Y-D. Z., X-S. L., Z-J. Y., H-M. S. and J-X. W. collected the sera samples. X-L F., Y. L.,
504 M-L. M., Z-W. X., B. Z., H. C., C-Z. Y., J-B. X., X-N. W., Y-X. Z., D-Y. L., H-N. Z.,
505 H-W. J., H. Q., and S-J. G. performed the microarray experiments and data analysis.
506 H-P.W., W.H. and Y-N.Z. performed the neutralization assay. S-C.T., Y. L. and M-L. M.
507 wrote the manuscript with suggestions from other authors.

508

509 **Competing interests:**

510 The authors declare no competing interests.

511

512

513 **Main figure titles and legends**

514

515 **Figure 1. The IgG linear epitope landscape of the SARS-CoV-2 Spike protein. A.**

516 The signal intensities of 1,051 COVID-19 sera against 197 peptides were obtained by
517 using the peptide microarray. The peptides are listed in the X-axis and aligned to the
518 corresponding locations on the Spike protein. As a control, the signal intensities of the S1
519 protein were also presented. The missing spots are peptides that either could not be
520 synthesized or failed the BSA conjugation (see **Table S1** for details). A cohort of 528
521 control sera were also analysed on the microarray. In addition, the known
522 N-glycosylation sites (N-glyco) were aligned with the Spike protein. The peptides or
523 regions with significant binding were marked blue. Peptide S1-88 was specifically
524 labelled because significant bindings were also observed for the controls. SP: signalling

525 peptide; NTD: N-terminal domain; RBD: receptor binding domain; RBM: receptor binding
 526 motif; CTD1: C-terminal domain 1; CTD2: C-terminal domain 2; S2': protease cleavage
 527 site; FP: fusion peptide; FPPR: fusion peptide proximal region; HR1: heptad repeat 1;
 528 HR2: heptad repeat 2; CH: centre helix; CD: connector domain; TM: trans-membrane;
 529 CP: cytoplasmic. **B.** The area of solvent accessibility (ASA) of each amino acid for S1-93
 530 and S2-16, with regard to the S protein trimer structure (PDB: 6X6P). **C.** The response
 531 frequencies of the two groups of peptides with or without the glycosylation site. The P
 532 value was calculated with the t -test. **D.** The response frequency for each peptide in the
 533 two groups as S1-93 IgG positive or negative. The P value was calculated with the χ^2 test.
 534 *, $P < 0.05$; **, $P < 0.01$; ***, $P < 0.001$; ****, $P < 0.0001$; ns, not significant. **E.**
 535 Heatmap of Spearman's correlation coefficients between the IgG responses of the
 536 peptides and related proteins.

537

538 **Figure 2. Epitope numbers in patients are related with severity. A-B.** The distribution
 539 of the numbers of the responsive epitopes in both the COVID-19 ($n = 1,004$) and control
 540 groups ($n = 528$). For the COVID-19 group, samples collected less than 15 days after
 541 symptom onset were excluded. **C.** The numbers of the responsive epitopes in the three
 542 groups with regard to severity and outcome. **D.** The S1 IgG signal intensity of the
 543 samples with different numbers of the responsive epitopes. For **B-D**, the data were
 544 presented by mean + SD. P values were calculated using the two-sided t -test for others.
 545 For **C**, the P value was adjusted for multiple comparisons by BH (Benjamini and
 546 Hochberg) method.

547

548 **Figure 3. The IgG response of the epitopes is associated with severity. A.** The linear
 549 epitope landscape was divided into two sub-landscapes according to severity and
 550 outcome, *i.e.*, 517 non-severe, 455 severe (survivors) and 79 severe (non-survivors). The
 551 data are presented as the means \pm SD. **B-E.** IgG signal intensities (upper part) and
 552 response frequencies (lower part) of the three groups, *i.e.*, non-severe, severe (survivors)
 553 and severe (non-survivors) for the S1 protein (**E**), S1-93 (**F**), S1-97 (**G**), and S2-78 (**H**).
 554 The data were presented using the median with interquartile for the upper part, and
 555 response frequency with a 95% confidential interval for the lower part. P values were

556 calculated using the two-sided t-test for the upper part and the χ^2 test for the lower part
557 for **B-E**.

558

559 **Figure 4. RBD lacks highly immunogenic linear epitopes.** **A.** The RBD region of the
560 linear epitope landscape. **B.** The peptide microarray results of two Spike protein-specific
561 monoclonal human antibodies (from Active motif Co. Ltd.), one (414-1) is specific for
562 the RBD and the other (414-4) is not. **C.** Detailed structures of the significant epitopes
563 (S1-76/77/78, aa451-474, red) on the RBD of the closed-state Spike protein trimer, side
564 view (PDB ID: 6X6P). **D.** The locations of the significant epitopes s (S1-76/77/78,
565 aa451-474, red) on the co-crystal structure of the RBD and ACE2 (PDB ID: 6M0J). **E.**
566 Homology analysis of the significant epitopes, s, among the 7 known human
567 coronaviruses and bat coronavirus BtCoV-RaTG13, which is highly homologous to
568 SARS-CoV-2. Amino acids with consistencies $\geq 50\%$ among the 8 coronaviruses are
569 marked in red, and the loop and β -strand region are shown as a line and an arrow above
570 the sequences, respectively.

571

572 **Figure 5. CTD is rich in significant linear epitopes.** **A.** The CTD region of the linear
573 epitope landscape. **B.** The locations of the significant epitopes, s, are located on the CTD
574 (PDB ID: 6X6P). Specifically, S1-93, aa553-564, red; S1-97, aa577-588, blue;
575 S1-105/106, aa625-642, yellow; S1-111, aa661-672, green; and S1-113, S1-113, 673-684,
576 orange. **C.** Homology analysis of the significant epitopes s among the 7 known human
577 coronaviruses and bat coronavirus BtCoV-RaTG13. Amino acids with
578 consistencies $\geq 50\%$ among the 8 coronaviruses are marked in red, and the loop, α -helix
579 and β -strand region are shown as a line, a coil and an arrow above the sequences,
580 respectively. An unobserved structure is shown as a dotted line.

581

582 **Figure 6.** Dynamic changes in IgG responses to the epitopes. **A-H.** Median signal
583 intensity (left) and response frequency (right) of the samples collected at the indicated
584 time points, *i.e.*, collection_time or days after symptom onset for the indicated epitopes.

585

586 **Figure 7.** Neutralizing activities of the antibodies elicited by the linear epitopes in mice.
587 **A.** The workflow to generate and collect anti-sera from immunized mice for the peptides.
588 KLH only was used as a control. **B.** The specificity of the sera was monitored using a
589 peptide microarray containing the S protein, the RBD and all the peptides that cover the
590 entire S protein. Some representative results are shown. **C.** Summary of the neutralization
591 activity of the peptide-immunized antibodies in mouse sera (n=3). The sera were diluted
592 1:10. P values were calculated by one-way ANOVA test. *****, $P < 0.0001$; ns, not
593 significant. **D.** Representative results of the neutralization activity (top) and morphology
594 of plaques (bottom). Sera were serial diluted at a range from 1:10 to 1:80.

595

596

597

598 **STAR Methods**

599

600 **RESOURCE AVAILABILITY**601 *Lead Contact*

602 Further information and requests for resources and reagents should be directed to and will
603 be fulfilled by the Lead Contact, Sheng-ce Tao (taosc@sjtu.edu.cn).

604

605 *Materials Availability*

606 This study did not generate new unique reagents.

607

608 *Data and Code Availability*

609 The peptide microarray data generated during this study are entered in the Protein
610 Microarray Database (<http://www.proteinmicroarray.cn>) under accession number
611 PMDE243. Additional Supplemental Items are available from Mendeley Data at
612 <http://dx.doi.org/10.17632/jxdg9kgnxf.1>. Additional data related to this paper may be
613 requested from the authors.

614

615 **EXPERIMENTAL MODEL AND SUBJECT DETAILS**

616 Patients and samples

617 The study was approved by the Ethical Committee of Tongji Hospital, Tongji Medical
618 College, Huazhong University of Science and Technology, Wuhan, China (IRB
619 ID:TJ-C20200128). Written informed consent was obtained from all participants enrolled
620 in this study. COVID-19 patients were hospitalized and received treatment in Tongji
621 Hospital from 17 February 2020 to 28 April 2020. Of the 1,051 patients, 523 are males
622 and 528 are females and the mean age of these patients is 60.3 with 614 patients over
623 60-year-old (**Table S2**). The basic criteria to define the severity, *i.e.*, mild, moderate,
624 severe and critically severe, are according to the Diagnosis and Treatment Protocol for
625 Novel Coronavirus Pneumonia (Trial Version 7), released by the National Health
626 Commission & State Administration of Traditional Chinese Medicine. Non-severe
627 patients are those with mild or moderate symptoms, while severe patients are those with
628 severe or critically severe symptoms. Sera were collected during hospitalization at viable
629 time points (**Table S2**). Sera from the control group of healthy donors, lung cancer
630 patients, and patients with autoimmune diseases were collected from Ruijin Hospital,
631 Shanghai, China or Tongren Hospital, Shanghai, China. All the sera were stored at -80°C
632 until use.

633

634 Peptide synthesis and conjugation with BSA

635 The N-terminal amidated peptides were synthesized using GL Biochem, Ltd. (Shanghai,
636 China). Each peptide was individually conjugated with BSA using Sulfo-SMCC (Thermo
637 Fisher Scientific, MA, USA), according to the manufacturer's instructions. Briefly, BSA
638 was activated by Sulfo-SMCC in a molar ratio of 1: 30, followed by dialysis in PBS
639 buffer. Peptides containing cysteine were added in a w/w ratio of 1:1 and incubated for 2
640 h, followed by dialysis in PBS to remove free peptides. A few conjugates were randomly
641 selected for examination by SDS-PAGE. For conjugates of the biotin-BSA-peptide,
642 before conjugation, BSA was labelled with biotin using the NHS-LC-Biotin reagent
643 (Thermo Fisher Scientific, MA, USA) at a molar ratio of 1: 5 and then activated using
644 Sulfo-SMCC.

645

646 METHOD DETAILS**647 Peptide microarray fabrication**

648 The peptide-BSA conjugates and S1 protein, the RBD protein and N protein of
649 SARS-CoV-2, along with the negative (BSA) and positive controls (anti-human IgG and
650 IgM antibodies), were printed in triplicate on a PATH substrate slide (Grace Bio-Labs,
651 Oregon, USA) to generate identical arrays in a 1 x 7 subarray format using a Super
652 Marathon printer (Arrayjet, UK). The microarrays were stored at -80°C until use.

653

654 Microarray-based serum analysis

655 A 14-chamber rubber gasket was mounted onto each slide to create individual chambers
656 for the 14 identical subarrays. The microarray was used for serum profiling as previously
657 described with minor modifications (Li et al., 2020b). Briefly, the arrays stored at -80°C
658 were warmed to room temperature and then incubated in blocking buffer (3% BSA in
659 1×PBS buffer with 0.1% Tween 20) for 3 h. A total of 200 µL of diluted sera or
660 antibodies was incubated with each subarray for 2 h. The sera were diluted at 1:200 for
661 most samples, and for the competition experiment, free peptides were added at a
662 concentration of 0.25 mg/mL. For the enriched antibodies, 0.1-0.5 µg antibodies were
663 included in the 200 µL incubation buffer. The arrays were washed with 1×PBST, and
664 bound antibodies were detected by incubating with Cy3-conjugated goat anti-human IgG
665 and Alexa Fluor 647-conjugated donkey anti-human IgM (Jackson ImmunoResearch, PA,
666 USA), which were diluted at 1: 1,000 in 1×PBST. The incubation was carried out at room
667 temperature for 1 h. The microarrays were then washed with 1×PBST and dried by
668 centrifugation at room temperature and scanned using a LuxScan 10K-A (CapitalBio
669 Corporation, Beijing, China), with the parameters set at 95% laser power/PMT 550 and
670 95% laser power/PMT 480 for IgM and IgG, respectively. The fluorescent intensity was
671 determined using GenePix Pro 6.0 software (Molecular Devices, CA, USA).

672

673 Mouse immunization

674 The peptides were synthesized and coupled to KLH through SMCC (Thermo Fisher
675 Scientific, MA, USA) by GL Biochem Ltd. (Shanghai, China). For each peptide, three
676 female mice (BALB/c) approximately 6 ~ 8 weeks old were immunized four times on a
677 weekly schedule, and 50 µg KLH conjugated peptide was mixed with 60 µg manganese
678 salt (MnJ) adjuvants (Zhang et al., 2019) for each immunization through intraperitoneal
679 (IP) injections. Serum samples were collected 7 d after each immunization for microarray
680 and neutralization assays.

681

682 **Cell lines and viruses**

683 Vero E6 cells (ATCC CRL-1586) were grown in Dulbecco's modified Eagle's medium
684 (DMEM) supplemented with 100 µg/mL streptomycin and 100 U/mL penicillin, 10%
685 FBS (Sigma-Aldrich, USA), and maintained at 37°C with 5% CO₂. SARS-CoV-2
686 (nCoV-2019BetaCoV/Wuhan/WIV04/2019) was obtained from the National Virus
687 Resource, Wuhan Institute of Virology, Chinese Academy of Sciences. All handling of
688 the virus was conducted in a BSL-3 laboratory.

689

690 **Plaque reduction neutralization assay**

691 For the plaque reduction neutralization test, Vero E6 cells were grown to confluence in a
692 12-well plate (Corning, USA) at 37°C, 5% CO₂, overnight. Additionally, 300 µL twofold
693 serial diluted serum samples from 1:10 to 1:80 were prepared in 2.5% FBS-DMEM. The
694 live SARS-CoV-2 virus (300 PFU/mL) was added into the serum at a 1:1 volume, mixed
695 completely, and incubated at 37°C for 1 h. Then, cell culture media were removed from
696 the 12-well plates, and 500 µL of serum-virus mixture was added to each cell. After
697 incubation at 37°C for 1 h, the mixture was replaced with 1000 µL 2.5% FBS-DMEM
698 containing 0.8% carboxymethylcellulose (Sigma-Aldrich, USA). Four days later, the
699 plates were fixed with 8% paraformaldehyde and stained with 0.5% crystal violet.
700 Neutralizing antibody CB6 (Shi et al., 2020) of SARS-CoV-2 was used as the positive
701 control. The antibody was provided by Prof. Jing-Hua Yan at the Institute of
702 Microbiology, Chinese Academy of Sciences.

703

704

705 **QUANTIFICATION AND STATISTICAL ANALYSIS**706 **Data analysis of peptide microarray**

707 For each spot, signal intensity was defined as the mean_foreground subtracted by the
708 mean_background. The signal intensities of the triplicate spots for each peptide or protein
709 were averaged. The overall_mean_background and the overall_standard deviation
710 (SD)_background of all the arrays probed with COVID-19 sera were calculated. Cutoff1
711 was defined as (the overall_mean_background + 2*overall_SD_background). According
712 to the array data, Cutoff1 was calculated as 380.7. For the control arrays,
713 mean_foreground and SD_foreground for each peptide and protein were calculated.
714 Cutoff2 was set as (control_mean_signal intensity + 2*control_SD_signal intensity). For
715 each peptide or protein, a SARS-CoV-2-specific positive response was called when the
716 average_signal intensity was larger than both Cutoff1 and Cutoff2. Response frequency
717 was then defined as the number of peptides with a positive response divided by the total
718 number of peptides on the microarray.

719

720 **Structure analysis**

721 The spike protein structures (PDB ID: 6X6P and 6VYB), RBD-ACE2 structure (PDB ID:
722 6M0J) and antibody-RBD complex structure (PDB ID: 7C01, 7BWJ, 7BYR, 6W41 and
723 6WPT) were used to analyse the structural details of the epitopes identified from the
724 peptide microarray. The C terminal (1146-1273) structure of the Spike protein came from
725 a modelling structure, QHD43416.pdb, generated by C-I-TASSER
726 (<https://zhanglab.ccmb.med.umich.edu/COVID-19/>) and aligned to the C terminus of the
727 Spike protein (PDB ID: 6X6P). Structural analysis was processed in Pymol. The
728 alignment and homology analysis of 7 human coronaviruses and one bat coronavirus was
729 generated using the ClustalW algorithm from EMBL-EBI
730 (<https://www.ebi.ac.uk/Tools/msa/clustalo/>).

731

732

733

734 **Supplemental item titles**

735 **Table S1. Reactivity of all the peptides on the microarray (related to Figure 1 and**
736 **Figure S1).**

737 **Table S2. Serum samples tested in this study (related to Figure 1).**

738 **Table S3. Highly immunogenic epitopes (related to Figure 1).**

739 **Table S4. Epitope map on S protein 3D structures from more resources (related to**
740 **Figure 1).**

741 **Table S5. Statistical analysis of the IgG responses against the significant epitopes**
742 **and S1 protein related to gender, age, severity and NAT (related to Figure 3).**

743 **Table S6. Clinical parameters that are correlated with antibody response (related to**
744 **Figure 3).**

745 **Table S7. Structural analysis of reported neutralizing antibodies binding with the S**
746 **protein (related to Figure 4).**

747

748

749

750

751 **References**

752

753 Abbott, R.K., and Crotty, S. (2020). Factors in B cell competition and immunodominance.
754 *Immunol. Rev.* 296, 120–131.

755 Ahmed, S.F., Quadeer, A.A., and McKay, M.R. (2020). COVIDep: A web-based
756 platform for real-time reporting of vaccine target recommendations for SARS-CoV-2.
757 *Nat. Protoc.* 15, 2141–2142.

758 Andersen, K.G., Rambaut, A., Lipkin, W.I., Holmes, E.C., and Garry, R.F. (2020). The
759 proximal origin of SARS-CoV-2. *Nat. Med.* 26, 450–452.

760 Baden, L.R., El Sahly, H.M., Essink, B., Kotloff, K., Frey, S., Novak, R., Diemert, D.,
761 Spector, S.A., Rouphael, N., Creech, C.B., et al. (2020). Efficacy and Safety of the
762 mRNA-1273 SARS-CoV-2 Vaccine. *N. Engl. J. Med.*

763 Barnes, C.O., Jette, C.A., Abernathy, M.E., Dam, K.-M.A., Esswein, S.R., Gristick, H.B.,
764 Maljutin, A.G., Sharaf, N.G., Huey-Tubman, K.E., Lee, Y.E., et al. (2020).
765 SARS-CoV-2 neutralizing antibody structures inform therapeutic strategies. *Nature* DOI:
766 10.1038/s41586-020-2852-1.

767 Baum, A., Fulton, B.O., Wloga, E., Copin, R., Pascal, K.E., Russo, V., Giordano, S.,
768 Lanza, K., Negron, N., Ni, M., et al. (2020). Antibody cocktail to SARS-CoV-2 spike
769 protein prevents rapid mutational escape seen with individual antibodies. *Science* (80-.).
770 eabd0831.

- 771 Boyd, S.D., and Jackson, K.J.L. (2015). Predicting vaccine responsiveness. *Cell Host*
772 *Microbe* *17*, 301–307.
- 773 Cai, Y., Yin, D., Ling, S., Tian, X., Li, Y., Xu, Z., Jiang, H., Zhang, X., Wang, X., Shi,
774 Y., et al. (2020). A single dose SARS-CoV-2 simulating particle vaccine induces potent
775 neutralizing activities. *BioRxiv* DOI: 10.1101/2020.05.14.093054.
- 776 Cao, Y., Su, B., Guo, X., Sun, W., Deng, Y., Bao, L., Zhu, Q., Zhang, X., Zheng, Y.,
777 Geng, C., et al. (2020). Potent neutralizing antibodies against SARS-CoV-2 identified by
778 high-throughput single-cell sequencing of convalescent patients' B cells. *Cell* *182*,
779 73-84.e16.
- 780 Chi, X., Yan, R., Zhang, J., Zhang, G., Zhang, Y., Hao, M., Zhang, Z., Fan, P., Dong, Y.,
781 Yang, Y., et al. (2020). A neutralizing human antibody binds to the N-terminal domain of
782 the Spike protein of SARS-CoV-2. *Science* (80-.). *369*, 650–655.
- 783 Cirelli, K.M., Carnathan, D.G., Nogal, B., Martin, J.T., Rodriguez, O.L., Upadhyay, A.A.,
784 Enemuo, C.A., Gebru, E.H., Choe, Y., Viviano, F., et al. (2019). Slow Delivery
785 Immunization Enhances HIV Neutralizing Antibody and Germinal Center Responses
786 via Modulation of Immunodominance. *Cell* *177*, 1153-1171.e28.
- 787 Custódio, T.F., Das, H., Sheward, D.J., Hanke, L., Pazicky, S., Pieprzyk, J., Sorgenfrei,
788 M., Schroer, M.A., Gruzinov, A.Y., Jeffries, C.M., et al. (2020). Selection, biophysical
789 and structural analysis of synthetic nanobodies that effectively neutralize SARS-CoV-2.
790 *Nat. Commun.* *11*, 5588.
- 791 Dong, E., Du, H., and Gardner, L. (2020a). An interactive web-based dashboard to track
792 COVID-19 in real time. *Lancet Infect. Dis.* *20*, 533–534.
- 793 Dong, Y., Dai, T., Wei, Y., Zhang, L., Zheng, M., and Zhou, F. (2020b). A systematic
794 review of SARS-CoV-2 vaccine candidates. *Signal Transduct. Target. Ther.* *5*, 237.
- 795 Du, S., Cao, Y., Zhu, Q., Yu, P., Qi, F., Wang, G., Du, X., Bao, L., Deng, W., Zhu, H., et
796 al. (2020). Structurally Resolved SARS-CoV-2 Antibody Shows High Efficacy in
797 Severely Infected Hamsters and Provides a Potent Cocktail Pairing Strategy. *Cell* *183*,
798 1013-1023.e13.
- 799 Emini, E.A., Hughes, J. V, Perlow, D.S., and Boger, J. (1985). Induction of hepatitis A
800 virus-neutralizing antibody by a virus-specific synthetic peptide. *J. Virol.* *55*, 836–839.
- 801 Hanke, L., Vidakovics Perez, L., Sheward, D.J., Das, H., Schulte, T., Moliner-Morro, A.,
802 Corcoran, M., Achour, A., Karlsson Hedestam, G.B., Hällberg, B.M., et al. (2020). An
803 alpaca nanobody neutralizes SARS-CoV-2 by blocking receptor interaction. *Nat.*
804 *Commun.* *11*, 4420.
- 805 Hansen, J., Baum, A., Pascal, K.E., Russo, V., Giordano, S., Wloga, E., Fulton, B.O.,
806 Yan, Y., Koon, K., Patel, K., et al. (2020a). Studies in humanized mice and convalescent
807 humans yield a SARS-CoV-2 antibody cocktail. *Science* (80-.). eabd0827.
- 808 Hansen, J., Baum, A., Pascal, K.E., Russo, V., Giordano, S., Wloga, E., Fulton, B.O.,
809 Yan, Y., Koon, K., Patel, K., et al. (2020b). Studies in humanized mice and convalescent
810 humans yield a SARS-CoV-2 antibody cocktail. *Science* (80-.). *369*, 1010–1014.
- 811 Haynes, B.F., Corey, L., Fernandes, P., Gilbert, P.B., Hotez, P.J., Rao, S., Santos, M.R.,
812 Schuitemaker, H., Watson, M., and Arvin, A. (2020). Prospects for a safe COVID-19
813 vaccine. *Sci. Transl. Med.* *12*.
- 814 Herrera, N.G., Morano, N.C., Celikgil, A., Georgiev, G.I., Malonis, R.J., Lee, J.H., Tong,
815 K., Vergnolle, O., Massimi, A.B., Yen, L.Y., et al. (2020). Characterization of the

- 816 SARS-CoV-2 S Protein: Biophysical, Biochemical, Structural, and Antigenic Analysis.
817 BioRxiv DOI: 10.1101/2020.06.14.150607.
- 818 Huang, C., Wang, Y., Li, X., Ren, L., Zhao, J., Hu, Y., Zhang, L., Fan, G., Xu, J., and Gu,
819 X. (2020). Clinical features of patients infected with 2019 novel coronavirus in Wuhan ,
820 China. *Lancet* 6736, 1–10.
- 821 Hurlburt, N.K., Seydoux, E., Wan, Y.-H., Edara, V.V., Stuart, A.B., Feng, J., Suthar,
822 M.S., McGuire, A.T., Stamatatos, L., and Pancera, M. (2020). Structural basis for potent
823 neutralization of SARS-CoV-2 and role of antibody affinity maturation. *Nat. Commun.*
824 11, 5413.
- 825 Iyer, A.S., Jones, F.K., Nodoushani, A., Kelly, M., Becker, M., Slater, D., Mills, R., Teng,
826 E., Kamruzzaman, M., Garcia-Beltran, W.F., et al. (2020). Persistence and decay of
827 human antibody responses to the receptor binding domain of SARS-CoV-2 spike
828 protein in COVID-19 patients. *Sci. Immunol.* 5.
- 829 Jeyanathan, M., Afkhami, S., Smaill, F., Miller, M.S., Lichty, B.D., and Xing, Z. (2020).
830 Immunological considerations for COVID-19 vaccine strategies. *Nat. Rev. Immunol.* 20,
831 615–632.
- 832 Jiang, H., Li, Y., Zhang, H., Wang, W., Men, D., Yang, X., Qi, H., Zhou, J., and Tao, S.
833 (2020a). SARS-CoV-2 proteome microarray for global profiling of COVID-19 specific
834 IgG and IgM responses. *Nat. Commun.* 11, 3581.
- 835 Jiang, S., Hillyer, C., and Du, L. (2020b). Neutralizing Antibodies against SARS-CoV-2
836 and Other Human Coronaviruses. *Trends Immunol.* 41, 355–359.
- 837 Ju, B., Zhang, Q., Ge, J., Wang, R., Sun, J., Ge, X., Yu, J., Shan, S., Zhou, B., Song, S.,
838 et al. (2020). Human neutralizing antibodies elicited by SARS-CoV-2 infection. *Nature*
839 584, 115–119.
- 840 Korber, B., Fischer, W.M., Gnanakaran, S., Yoon, H., Theiler, J., Abfalterer, W.,
841 Hengartner, N., Giorgi, E.E., Bhattacharya, T., Foley, B., et al. (2020). Tracking changes
842 in SARS-CoV-2 Spike: evidence that D614G increases infectivity of the COVID-19 virus.
843 *Cell* DOI: 10.1016/j.cell.2020.06.043.
- 844 Krammer, F. (2020). SARS-CoV-2 vaccines in development. *Nature* 586, 516–527.
- 845 Kreye, J., Reincke, S.M., Kornau, H.-C., Sánchez-Sendin, E., Corman, V.M., Liu, H.,
846 Yuan, M., Wu, N.C., Zhu, X., Lee, C.-C.D., et al. (2020). A Therapeutic
847 Non-self-reactive SARS-CoV-2 Antibody Protects from Lung Pathology in a
848 COVID-19 Hamster Model. *Cell* 183, 1058-1069.e19.
- 849 Kyte, J., and Doolittle, R.F. (1982). A simple method for displaying the hydrophobic
850 character of a protein. *J. Mol. Biol.* 157, 105–132.
- 851 Larman, H.B., Zhao, Z., Laserson, U., Li, M.Z., Ciccia, A., Gakidis, M.A.M., Church,
852 G.M., Kesari, S., Leproust, E.M., Solimini, N.L., et al. (2011). Autoantigen discovery
853 with a synthetic human peptidome. *Nat. Biotechnol.* 29, 535–541.
- 854 Li, Y., Lai, D., Zhang, H., Jiang, H., Tian, X., Ma, M., Qi, H., Meng, Q., Guo, S., Wu, Y.,
855 et al. (2020a). Linear epitopes of SARS-CoV-2 spike protein elicit neutralizing antibodies
856 in COVID-19 patients. *Cell. Mol. Immunol.* 17, 1095–1097.
- 857 Li, Y., Li, C.-Q., Guo, S.-J., Guo, W., Jiang, H.-W., Li, H.-C., and Tao, S.-C. (2020b).
858 Longitudinal serum autoantibody repertoire profiling identifies surgery-associated
859 biomarkers in lung adenocarcinoma. *EBioMedicine* 53, 102674.

860 Liu, L., Wei, Q., Lin, Q., Fang, J., Wang, H., Kwok, H., Tang, H., Nishiura, K., Peng, J.,
861 Tan, Z., et al. (2019). Anti-spike IgG causes severe acute lung injury by skewing
862 macrophage responses during acute SARS-CoV infection. *JCI Insight* 4, e123158.

863 Liu, L., Wang, P., Nair, M.S., Yu, J., Rapp, M., Wang, Q., Luo, Y., Chan, J.F.-W., Sahi,
864 V., Figueroa, A., et al. (2020). Potent neutralizing antibodies against multiple epitopes on
865 SARS-CoV-2 spike. *Nature* 584, 450–456.

866 Liu, S., Xiao, G., Chen, Y., He, Y., Niu, J., Escalante, C.R., Xiong, H., Farmar, J.,
867 Debnath, A.K., Tien, P., et al. (2004). Interaction between heptad repeat 1 and 2 regions
868 in spike protein of SARS-associated coronavirus: Implications for virus fusogenic
869 mechanism and identification of fusion inhibitors. *Lancet* 363, 938–947.

870 Long, Q.X., Liu, B.Z., Deng, H.J., Wu, G.C., Deng, K., Chen, Y.K., Liao, P., Qiu, J.F.,
871 Lin, Y., Cai, X.F., et al. (2020a). Antibody responses to SARS-CoV-2 in patients with
872 COVID-19. *Nat. Med.* 26, 845–848.

873 Long, Q.X., Tang, X.J., Shi, Q.L., Li, Q., Deng, H.J., Yuan, J., Hu, J.L., Xu, W., Zhang,
874 Y., Lv, F.J., et al. (2020b). Clinical and immunological assessment of asymptomatic
875 SARS-CoV-2 infections. *Nat. Med.* 26, 1200–1204.

876 Lv, Z., Deng, Y.-Q., Ye, Q., Cao, L., Sun, C.-Y., Fan, C., Huang, W., Sun, S., Sun, Y.,
877 Zhu, L., et al. (2020). Structural basis for neutralization of SARS-CoV-2 and SARS-CoV
878 by a potent therapeutic antibody. *Science* (80-.). 369, 1505–1509.

879 Mehta, P., McAuley, D.F., Brown, M., Sanchez, E., Tattersall, R.S., and Manson, J.J.
880 (2020). COVID-19: consider cytokine storm syndromes and immunosuppression. *Lancet*
881 395, 1033–1034.

882 Piccoli, L., Park, Y.-J., Tortorici, M.A., Czudnochowski, N., Walls, A.C., Beltramello,
883 M., Silacci-Fregni, C., Pinto, D., Rosen, L.E., Bowen, J.E., et al. (2020). Mapping
884 Neutralizing and Immunodominant Sites on the SARS-CoV-2 Spike Receptor-Binding
885 Domain by Structure-Guided High-Resolution Serology. *Cell* 183, 1024-1042.e21.

886 Pinto, D., Park, Y.-J., Beltramello, M., Walls, A.C., Tortorici, M.A., Bianchi, S., Jaconi,
887 S., Culap, K., Zatta, F., De Marco, A., et al. (2020). Structural and functional analysis of
888 a potent sarbecovirus neutralizing antibody. *BioRxiv* DOI: 10.1101/2020.04.07.023903.

889 Poh, C.M., Carissimo, G., Wang, B., Amrun, S.N., Lee, Y.-P., Chee, R.S.-L., Yeo,
890 N.K.-W., Lee, W.-H., Leo, Y.-S., Chen, M.I.-C., et al. (2020). Two linear epitopes on the
891 SARS-CoV-2 spike protein that elicit neutralising antibodies in COVID-19 patients. *Nat.*
892 *Commun.* 11, 2806.

893 Polack, F.P., Thomas, S.J., Kitchin, N., Absalon, J., Gurtman, A., Lockhart, S., Perez,
894 J.L., Pérez Marc, G., Moreira, E.D., Zerbini, C., et al. (2020). Safety and Efficacy of the
895 BNT162b2 mRNA Covid-19 Vaccine. *N. Engl. J. Med.* 383, 2603–2615.

896 Poland, G.A., Ovsyannikova, I.G., and Kennedy, R.B. (2020). SARS-CoV-2 immunity:
897 review and applications to phase 3 vaccine candidates. *Lancet* 396, 1595–1606.

898 Premkumar, L., Segovia-Chumbez, B., Jadi, R., Martinez, D.R., Raut, R., Markmann,
899 A.J., Cornaby, C., Bartelt, L., Weiss, S., Park, Y., et al. (2020). The receptor-binding
900 domain of the viral spike protein is an immunodominant and highly specific target of
901 antibodies in SARS-CoV-2 patients. *Sci. Immunol.* 5, eabc8413.

902 Rujas, E., Kucharska, I., Tan, Y.Z., Benlekbir, S., Cui, H., Zhao, T., Wasney, G.A.,
903 Budyłowski, P., Guvenc, F., Newton, J.C., et al. (2020). Multivalency transforms
904 SARS-CoV-2 antibodies into broad and ultrapotent neutralizers. *BioRxiv* DOI:
905 10.1101/2020.10.15.341636.

- 906 Schoof, M., Faust, B., Saunders, R.A., Sangwan, S., Rezelj, V., Hoppe, N., Boone, M.,
907 Billesbølle, C.B., Puchades, C., Azumaya, C.M., et al. (2020). An ultrapotent synthetic
908 nanobody neutralizes SARS-CoV-2 by stabilizing inactive Spike. *Science* (80-). DOI:
909 10.1126/science.abe3255.
- 910 Shi, R., Shan, C., Duan, X., Chen, Z., Liu, P., Song, J., Song, T., Bi, X., Han, C., Wu, L.,
911 et al. (2020). A human neutralizing antibody targets the receptor binding site of
912 SARS-CoV-2. *Nature* 584, 120–124.
- 913 Shi, X., Fan, X., Nie, S., Kou, L., Zhang, X., Liu, H., Ji, S., Deng, R., Wang, A., and
914 Zhang, G. (2019). Identification of a linear B-cell epitope on glycoprotein (GP) 2a of
915 porcine reproductive and respiratory syndrome virus (PRRSV). *Int. J. Biol. Macromol.*
916 139, 1288–1294.
- 917 Shrock, E., Fujimura, E., Kula, T., Timms, R.T., Lee, I.-H., Leng, Y., Robinson, M.L.,
918 Sie, B.M., Li, M.Z., Chen, Y., et al. (2020). Viral epitope profiling of COVID-19 patients
919 reveals cross-reactivity and correlates of severity. *Science* (80-). doi:
920 10.1126/science.abd4250.
- 921 Sikora, M., von Bülow, S., Blanc, F.E.C., Gecht, M., Covino, R., and Hummer, G. (2020).
922 Map of SARS-CoV-2 spike epitopes not shielded by glycans. *BioRxiv* DOI:
923 10.1101/2020.07.03.186825.
- 924 Tortorici, M.A., Beltramello, M., Lempp, F.A., Pinto, D., Dang, H. V, Rosen, L.E.,
925 McCallum, M., Bowen, J., Minola, A., Jaconi, S., et al. (2020). Ultrapotent human
926 antibodies protect against SARS-CoV-2 challenge via multiple mechanisms. *Science*
927 (80-). 370, 950–957.
- 928 Vabret, N., Britton, G.J., Gruber, C., Hegde, S., Kim, J., Kuksin, M., Levantovsky, R.,
929 Malle, L., Moreira, A., Park, M.D., et al. (2020). Immunology of COVID-19: Current
930 State of the Science. *Immunity* 52, 910–941.
- 931 Walls, A.C., Park, Y.J., Tortorici, M.A., Wall, A., McGuire, A.T., and Velesler, D. (2020).
932 Structure, Function, and Antigenicity of the SARS-CoV-2 Spike Glycoprotein. *Cell* 181,
933 281-292.e6.
- 934 Wan, J., Xing, S., Ding, L., Wang, Y., Zhu, D., Rong, B., Wang, S., Chen, K., He, C.,
935 Yuan, S., et al. (2020). Human IgG cell neutralizing monoclonal antibodies block SARS-
936 CoV-2 infection. *Cell Rep.* 32, 107918.
- 937 Wang, H., Hou, X., Wu, X., Liang, T., Zhang, X., Wang, D., Teng, F., Dai, J., Duan, H.,
938 Guo, S., et al. (2020a). SARS-CoV-2 proteome microarray for mapping COVID-19
939 antibody interactions at amino acid resolution. *ACS Cent. Sci.* 6, 2238-2249.
- 940 Wang, H., Hou, X., Wu, X., Liang, T., Zhang, X., Wang, D., Teng, F., Dai, J., Duan, H.,
941 Guo, S., et al. (2020b). SARS-CoV-2 proteome microarray for mapping COVID-19
942 antibody interactions at amino acid resolution. *BioRxiv* DOI:
943 10.1101/2020.03.26.994756.
- 944 Wang, Z., Li, Y., Hou, B., Pronobis, M.I., Wang, M., Wang, Y., Cheng, G., Weng, W.,
945 Wang, Y., Tang, Y., et al. (2020c). An array of 60,000 antibodies for proteome-scale
946 antibody generation and target discovery. *Sci. Adv.* 6, eaax2271.
- 947 Watanabe, Y., Allen, J.D., Wrapp, D., McLellan, J.S., and Crispin, M. (2020).
948 Site-specific glycan analysis of the SARS-CoV-2 spike. *Science* (80-). eabb9983.
- 949 Wec, A.Z., Wrapp, D., Herbert, A.S., Maurer, D.P., Haslwanter, D., Sakharkar, M.,
950 Jangra, R.K., Dieterle, M.E., Lilov, A., Huang, D., et al. (2020). Broad neutralization of
951 SARS-related viruses by human monoclonal antibodies. *Science* (80-). eabc7424.

- 952 Wu, C., Chen, X., Cai, Y., Xia, J., Zhou, X., Xu, S., Huang, H., Zhang, L., Zhou, X., Du,
953 C., et al. (2020a). Risk Factors Associated With Acute Respiratory Distress Syndrome
954 and Death in Patients With Coronavirus Disease 2019 Pneumonia in Wuhan, China.
955 *JAMA Intern. Med.* *180*, 934–943.
- 956 Wu, F., Zhao, S., Yu, B., Chen, Y.M., Wang, W., Song, Z.G., Hu, Y., Tao, Z.W., Tian,
957 J.H., Pei, Y.Y., et al. (2020b). A new coronavirus associated with human respiratory
958 disease in China. *Nature* *579*, 265–269.
- 959 Wu, N.C., Yuan, M., Liu, H., Lee, C.-C.D., Zhu, X., Bangaru, S., Torres, J.L., Caniels,
960 T.G., Brouwer, P.J.M., van Gils, M.J., et al. (2020c). An alternative binding mode of
961 IGHV3-53 antibodies to the SARS-CoV-2 receptor binding domain. *BioRxiv* DOI:
962 10.1101/2020.07.26.222232.
- 963 Wu, Y., Wang, F., Shen, C., Peng, W., Li, D., Zhao, C., Li, Z., Li, S., Bi, Y., Yang, Y., et
964 al. (2020d). A noncompeting pair of human neutralizing antibodies block COVID-19
965 virus binding to its receptor ACE2. *Science* (80-). *368*, 1274–1278.
- 966 Xu, G.J., Kula, T., Xu, Q., Li, M.Z., Vernon, S.D., Ndung'u, T., Ruxrungtham, K.,
967 Sanchez, J., Brander, C., Chung, R.T., et al. (2015). Comprehensive serological profiling
968 of human populations using a synthetic human virome. *Science* (80-). *384*, aaa0698.
- 969 Yuan, M., Wu, N.C., Zhu, X., Lee, C.C.D., So, R.T.Y., Lv, H., Mok, C.K.P., and Wilson,
970 I.A. (2020a). A highly conserved cryptic epitope in the receptor binding domains of
971 SARS-CoV-2 and SARS-CoV. *Science* (80-). *368*, 630–633.
- 972 Yuan, M., Liu, H., Wu, N.C., Lee, C.-C.D., Zhu, X., Zhao, F., Huang, D., Yu, W., Hua,
973 Y., Tien, H., et al. (2020b). Structural basis of a shared antibody response to
974 SARS-CoV-2. *Science* (80-). *369*, 1119–1123.
- 975 Zamecnik, C.R., Rajan, J. V, Yamauchi, K.A., Mann, S.A., Sowa, G.M., Zorn, K.C.,
976 Alvarenga, B.D., Stone, M., Norris, P.J., Gu, W., et al. (2020). ReScan, a Multiplex
977 Diagnostic Pipeline, Pans Human Sera for SARS-CoV-2 Antigens. *MedRxiv*
978 DOI:10.1101/2020.05.11.20092528.
- 979 Zhang, B., Hu, Y., Chen, L., Yau, T., Tong, Y., Hu, J., Cai, J., Chan, K.-H., Dou, Y.,
980 Deng, J., et al. (2020a). Mining of epitopes on spike protein of SARS-CoV-2 from
981 COVID-19 patients. *Cell Res.* *30*, 702–704.
- 982 Zhang, L., Jackson, C.B., Mou, H., Ojha, A., Rangarajan, E.S., Izard, T., Farzan, M., and
983 Choe, H. (2020b). The D614G mutation in the SARS-CoV-2 spike protein reduces S1
984 shedding and increases infectivity. *BioRxiv* DOI: 10.1101/2020.06.12.148726.
- 985 Zhang, R., Wang, C., Guan, Y., Wei, X., Sha, M., Jing, M., Lv, M., Xu, J., Wan, Y., and
986 Jiang, Z. (2019). The Manganese Salt (MnJ) Functions as A Potent Universal Adjuvant.
987 *BioRxiv* 783910.
- 988 Zhou, D., Duyvesteyn, H.M.E., Chen, C.-P., Huang, C.-G., Chen, T.-H., Shih, S.-R., Lin,
989 Y.-C., Cheng, C.-Y., Cheng, S.-H., Huang, Y.-C., et al. (2020a). Structural basis for the
990 neutralization of SARS-CoV-2 by an antibody from a convalescent patient. *Nat. Struct.*
991 *Mol. Biol.* *27*, 950–958.
- 992 Zhou, P., Yang, X. Lou, Wang, X.G., Hu, B., Zhang, L., Zhang, W., Si, H.R., Zhu, Y., Li,
993 B., Huang, C.L., et al. (2020b). A pneumonia outbreak associated with a new coronavirus
994 of probable bat origin. *Nature* *579*, 270–273.
- 995

In Brief

Li et al. construct a B cell linear epitope landscape of SARS-CoV-2 spike protein, based on a large cohort of COVID-19 patients. The epitope responses were related to disease severity and outcome but mainly elicit non-neutralizing antibodies.

Highlights

- A linear epitope landscape of the SARS-CoV-2 Spike from 1,051 COVID-19 patients
- Responsive epitopes are highly variable among patients and correlate with severity
- The RBD lacks linear epitopes but two other regions are rich in linear epitopes
- Little neutralization activity is observed for the linear epitope elicited antibodies

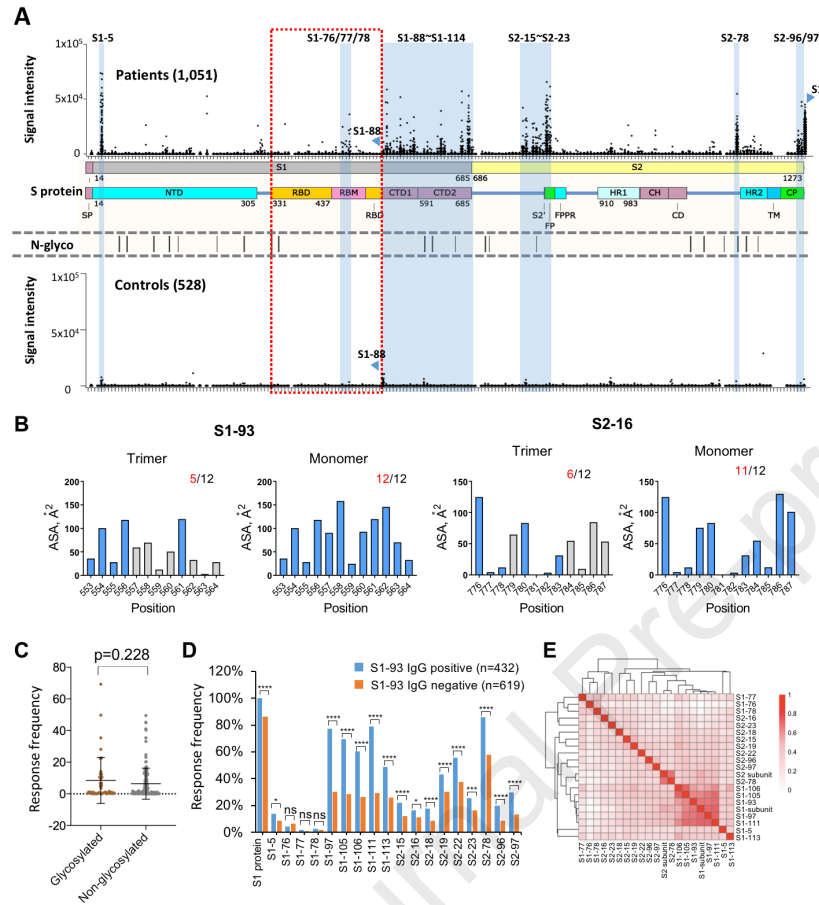


Figure 1. The IgG linear epitope landscape of the SARS-CoV-2 Spike protein.

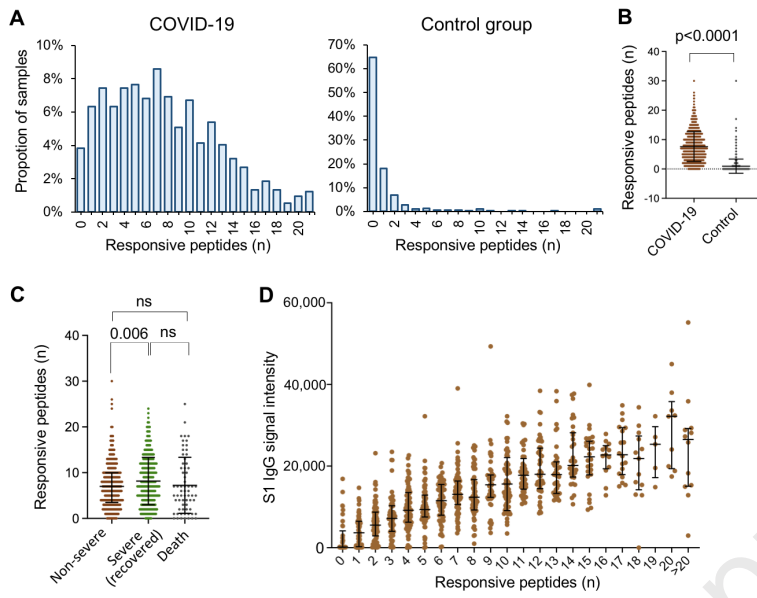


Figure 2. Epitope numbers in patients are related with severity.

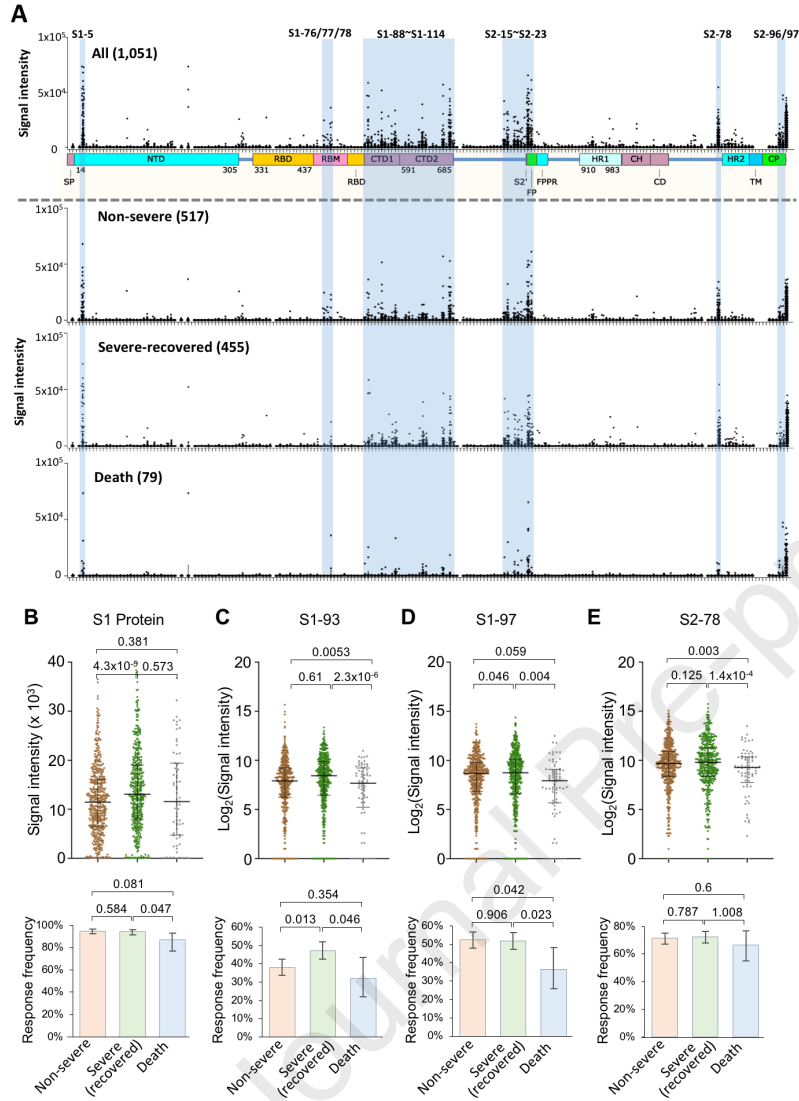


Fig. 3. The IgG response of the peptides is associated with severity

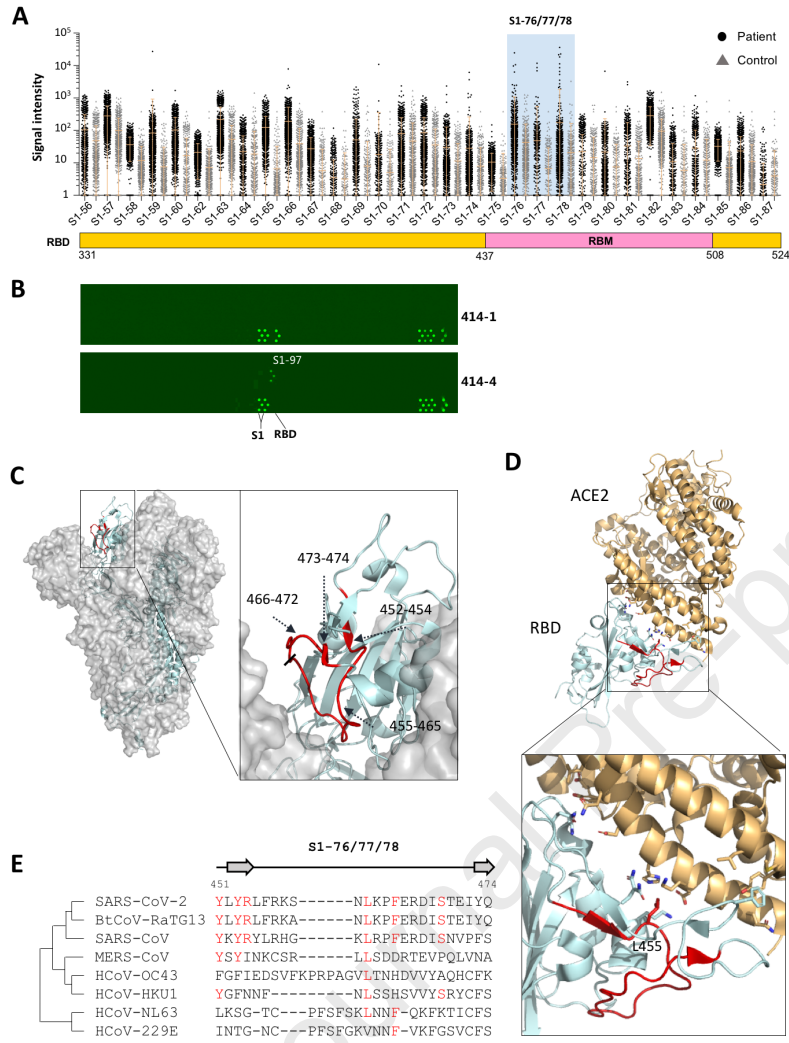


Figure 4. RBD lacks highly immunogenic linear epitopes.

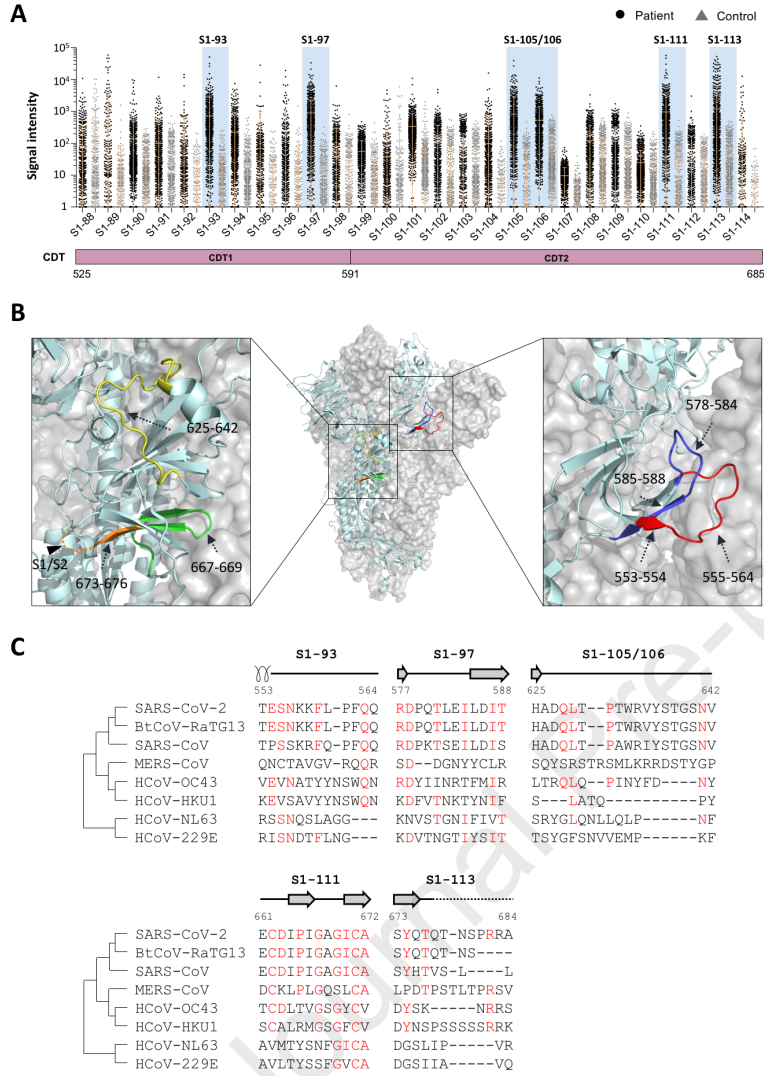


Figure 5. CTD is rich in significant linear epitopes.

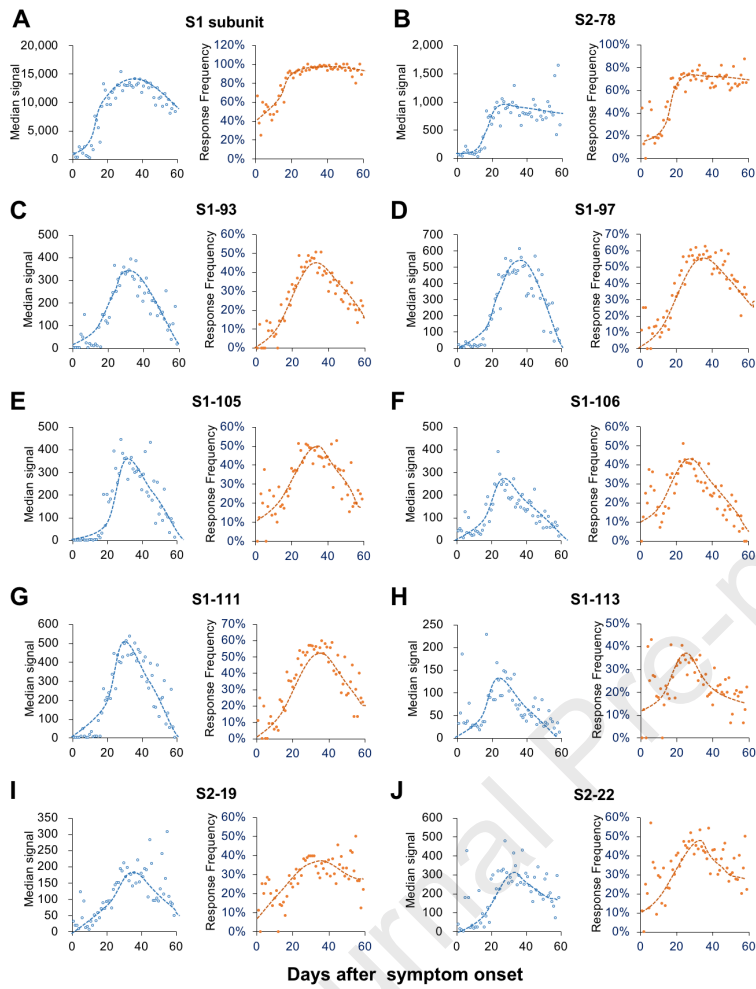


Fig. 6. Dynamic change of IgG response against the peptides

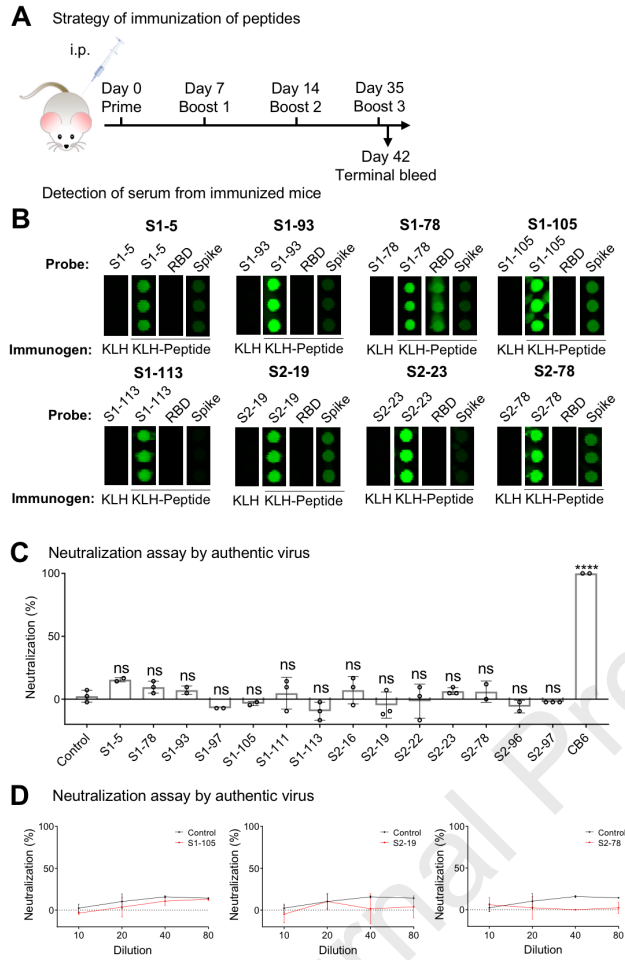


Figure 7. Neutralizing activities of the antibodies elicited by the linear epitopes in mice